Available online at www.sciencedirect.com
SCIENCE DIRECT®
Bioorganic & Medicinal Chemistry Letters 15 (2005) 3506–3509
Bioorganic & Medicinal Chemistry Letters

The molecular basis for coxib inhibition of p38α MAP kinase

Gilberto M. Sperandio da Silva,[a,b] Lidia M. Lima,[a] Carlos A. M. Fraga,[a] Carlos M. R. Sant'Anna[a,c] and Eliezer J. Barreiro[a,b,*]

[a]*Laboratório de Avaliação e Síntese de Substâncias Bioativas (LASSBio), Faculdade de Farmácia, Universidade Federal do Rio de Janeiro (UFRJ), Rio de Janeiro, PO Box 68006, RJ 21944-971, Brazil*
[b]*Departamento de Farmacologia Básica e Clínica, Instituto de Ciências Biomédicas, Universidade Federal do Rio de Janeiro (UFRJ), Rio de Janeiro, RJ, 21941-590, Brazil*
[c]*Departamento de Química, ICE, Universidade Federal Rural do Rio de Janeiro (UFRRJ), Seropédica, RJ 23851-970, Brazil*

Received 11 April 2005; revised 20 May 2005; accepted 26 May 2005

Abstract—In this work, we present the results of two combined approaches, molecular docking and comparative molecular field analysis (CoMFA), to propose how the selective cyclooxygenase-2 inhibitor celecoxib could act as a p38 mitogen-activated protein (MAP) kinase inhibitor. The docking analysis revealed why celecoxib has a less favorable binding energy ($\Delta G = -12.4$ kcal/mol) than the selective p38 MAP kinase (p38 MAPK) inhibitor, SB203580 ($\Delta G = -22.2$ kcal/mol). The CoMFA results revealed unfavorable steric effects that can be related to the predicted lower p38 MAP kinase inhibitory activity of celecoxib. Additionally, FlexX and CoMFA results also suggested that etoricoxib, another selective COX-2 inhibitor, could inhibit p38 MAP kinase.

Two important therapeutic targets to control chronic inflammatory response are mitogen-activated protein kinase (MAPK) and cyclooxygenase-2 (COX-2). MAP kinases are signaling molecules that are activated by a number of extracellular stress stimuli. The events that are regulated by p38 MAPK lead to the production of cytokines such as tumor necrosis factor-α (TNF-α) and interleukin-1β (IL-1β).[1] The pyridinyl-imidazoles represented by SB203580 were the first reported class of p38α inhibitors[1–3] (Fig. 1). Recently, some research groups have implemented efforts to develop new lead compounds to selectively inhibit p38 MAPK.[4–6] Moreover, COX-2 is selectively induced by proinflammatory cytokines (IL-1) and growth factors (TNF-α) and facilitates the release of prostaglandins involved in the evolution of the inflammatory process. Selective inhibitors of the COX-2 isoform represent a new generation of nonsteroidal anti-inflammatory drugs with a superior gastrointestinal safety profile.[7] Celecoxib was the first selective COX-2 inhibitor approved by FDA for the treatment of rheumatoid arthritis and osteoarthritis (Fig. 1).[8] Another important COX-2 selective inhibitor that still remains on the market is etoricoxib (Fig. 1).[9,10]

Additionally, it has been demonstrated that celecoxib can inhibit both catalytic activity and phosphorylation of p38 MAPK in models in vitro.[11] However, the molecular characteristics responsible for the inhibition of p38 MAPK still remain largely unsolved.

Some approaches have been applied as attempts to develop p38 MAPK QSAR models.[12,13] More recently, our research group has reported a 3D-QSAR study which applied the comparative molecular field analysis (CoMFA) methodology for dihydroquinazolinone and tetrasubstituted imidazole compounds known as p38 MAPK selective inhibitors.[14] Due to the structural similarity between celecoxib and p38 MAPK inhibitors, we were prompted to employ our QSAR 3D/CoMFA model as well as docking studies to better understand the structural characteristics involved in the molecular recognition of celecoxib by p38 MAPK.

The crystal structure of p38 MAPK in complex with inhibitor SB203580 was recovered from the Brookhaven Protein Data Bank (http://www.rcsb.org/pdb/) (entry code 1A9U). The X-ray crystal structure of COX-2 in complex with SC-558 (Fig. 1), a selective COX-2

Keywords: p38 MAPK inhibition; Coxib.
* Corresponding author. Tel.: +552125626644; Fax: +552125626644; e-mail: ejb@pharma.ufrj.br

0960-894X/$ - see front matter © 2005 Elsevier Ltd. All rights reserved.
doi:10.1016/j.bmcl.2005.05.107

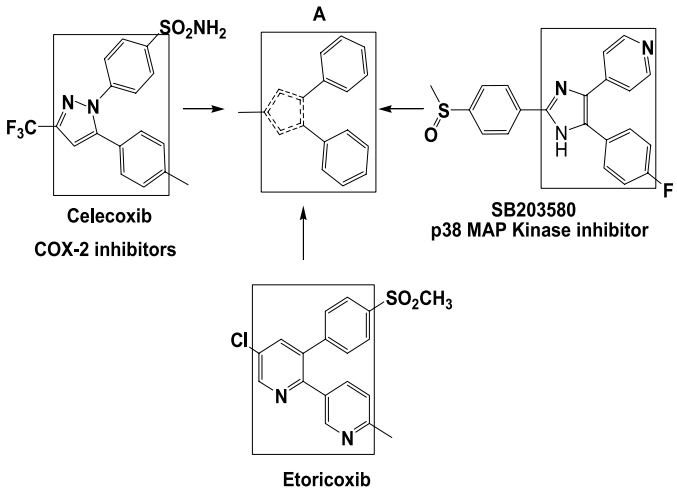

Figure 1. Common template between diarylheterocycle anti-inflammatory derivatives, celecoxib, etoricoxib, and SB203580.

inhibitor, was also recovered from the PDB (http://www.rcsb.org/pdb/) (entry code 1CX2). The conformation and orientation in the space of SC-558 extracted from the X-ray crystallographic inhibitor–enzyme complex were used as a template for the construction of celecoxib and etoricoxib, assuming that this conformation represents the most probable bioactive conformation of the compound at the enzyme active site level. The initial structures of the SB203580 and coxib compounds were generated by the molecular modeling software Sybyl 7.0. The geometries of these compounds were subsequently optimized using the Tripos force field with Gasteiger–Hückel charges.[15]

The FlexX program[16] interfaced with Sybyl 7.0 was used to dock the compounds celecoxib and SB203580 inside the active site of p38 MAPK. FlexX is an automated docking program that considers ligand conformational flexibility by an incremental fragment placing technique.[17] The active site for docking was defined as all atoms within 6.5 Å radius of the co-crystallized ligand. The proposed interaction mode of the ligands in the active site of p38 MAPK was determined as the highest scored conformation (best-fit ligand) among 30 conformational and binding modes generated according to FlexX scoring function, which is the structure with the most favorable free energy of binding, ΔG_{bind} (Fig. 2).

Chun et al.[11] have shown that celecoxib inhibited both the catalytic activity and the phosphorylation of p38 MAPK in experimentally induced carcinogenesis model, where they have found that celecoxib inhibited 12-*O*-tetradecanoylphorbol-13-acetate (TPA)-induced expression of COX-2 in female ICR mouse skin when applied topically 30 min prior to TPA as determined by both immunoblot and immunohistochemical analyses. This was the first evidence that a coxib could have pharmacological properties analogous to inhibitors of p38 MAPK, e.g., SB203580. Additionally, Müller has commented about the structural similarities between p38 MAPK and COX-2 inhibitors represented by coxib compounds and SB203580, where both have a common terphenylic-like template (A, Fig. 1).[18]

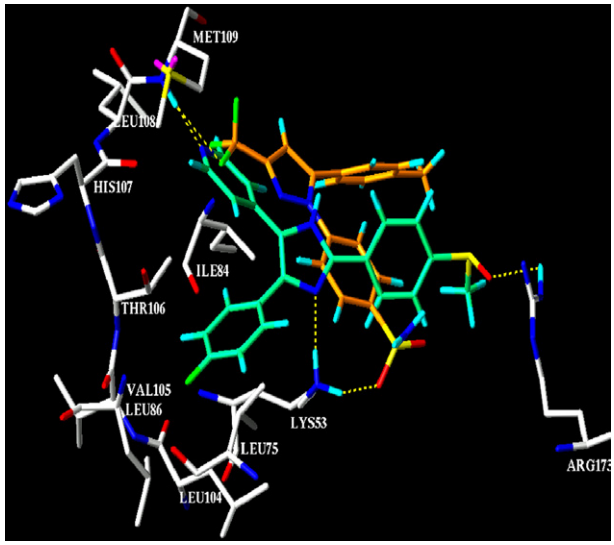

Figure 2. Probable binding conformation of celecoxib and its alignment in the binding site of p38 MAPK. FexX docking shows most important amino acid of p38 MAPK to interact with celecoxib. For celecoxib the carbon atoms are shown in orange (C), blue (N), red (O), and green (halogen). For SB203580, the carbon atoms are shown in green-blue (C), blue (N), red (O), and green (halogen).

To investigate the molecular characteristics of celecoxib possibly associated with the inhibition of p38 MAPK, we performed a modeling study using FlexX program to dock celecoxib into the active site of the enzyme. We also tested the p38 MAPK inhibitor SB203580 docking in the active site of p38 MAPK crystal structure to assess the efficiency of the program. FlexX docked the ligand in the same pocket as in the crystal structure and aligned the docked structure in a horizontal plane within the active site similar to that occupied by the bound ligand in the crystal structure (RMS value: 0.279 Å). Graphical representations of the docking results of both ligands are presented in Figure 2.

For SB203580, the ΔG_{bind} of the best-fit structure was −22.2 kcal/mol. As reported by Wang and colleagues,

the pyridine N atom of SB203580 is hydrogen bonded with the backbone amide of Met109 of p38 MAPK, an interaction that appears essential for binding.[3] Moreover, there is an interaction between the side-chain nitrogen atom of the conserved Lys53 and the N atom of the imidazole ring of compound SB203580.[3] The FlexX program could efficiently detect these interactions (Fig. 2). The program also detected an interaction between the side chain N–H of Arg173 and an O atom of methylsulfinyl moiety of SB203580.

After the docking procedure, the celecoxib molecule was located in the same pocket as SB203580, but in a different plane within the active site. The most favorable ΔG_{bind} observed was −12.4 kcal/mol. Comparing the ΔG_{bind} of celecoxib (−12.4 kcal/mol) with that of SB203590 (−22.2 kcal/mol), it can be predicted that celecoxib could inhibit p38 MAPK, but with a lower potency than SB203580. In fact, the concentration of celecoxib for the inhibition of p38 MAPK is 0.81 μM and the concentration of SB203580 for the inhibition of p38 MAPK is 0.048 μM.[3] Similar to SB203580, celecoxib is also interacting with two important amino acid residues, Met109 and Lys53. A fluorine atom of the trifluoromethyl group of celecoxib could accept a hydrogen bond from the backbone amide of Met109. A O atom of the sulfonamide group of celecoxib interacts with Lys53 (Fig. 2).

We employed our CoMFA model[14] for the prediction of the IC_{50} of SB203580 and celecoxib. The calculated IC_{50} of SB203580 was 0.072 μM, which is similar to the experimental IC_{50}, 0.048 μM.[3] Additionally, our CoMFA model[14] also predicts that celecoxib, which has a calculated IC_{50} = 0.81 μM, is less potent than SB203580 in the inhibition of p38 MAPK. To analyze structural characteristics associated to celecoxib activity, we compared the electrostatic and steric CoMFA contour maps with the structure of p38 MAPK in complex with celecoxib as recovered from the FlexX docking. Graphical representations of the CoMFA analysis results are displayed in Figure 3.

The electrostatic contour plots of CoMFA model were compared with the topology of celecoxib–p38 MAPK complexes (Fig. 3A). The electrostatic contour plots are displayed in blue and red contours. The red areas are regions where electron-rich groups are favorable to the inhibitory activity; the blue areas are regions where electron-poor groups are favorable to the inhibitory activity. Red contours near the sulfonamide and trifluoromethyl groups of celecoxib can be associated to the hydrogen bonds with the peptidic N–H group of residue Met109 and side-chain N–H group of residue Lys53 (Fig. 3A). However, it can also be observed that celecoxib has no groups associated to some electrostatic regions important for the p38 MAPK inhibitory activity.

The steric contour plots of celecoxib are displayed as green contours, which indicate regions where an increase in steric bulk will enhance activity, and yellow contours, which indicate regions where an increase in steric bulk will reduce activity. The large yellow contour near the celecoxib diaryl substitutes suggests that this is an unfavorable steric region which reduces the activity of celecoxib (Fig. 3B). On the other hand, important favorable steric regions were not observed near celecoxib, which could also be associated to its smaller activity compared to SB203580 (Fig. 3B).

The docking analysis and our CoMFA models were also used to predict binding affinity and the activity of etoricoxib (Table 1). Based on these results, we suggested that the p38 activity could be also inhibited by this other coxib derivative. In fact, it was observed that etoricoxib has more favorable ΔG_{bind}, and CoMFA model also predicts that it could be more potent than celecoxib (Table 1). Additionally, we were able to identify that

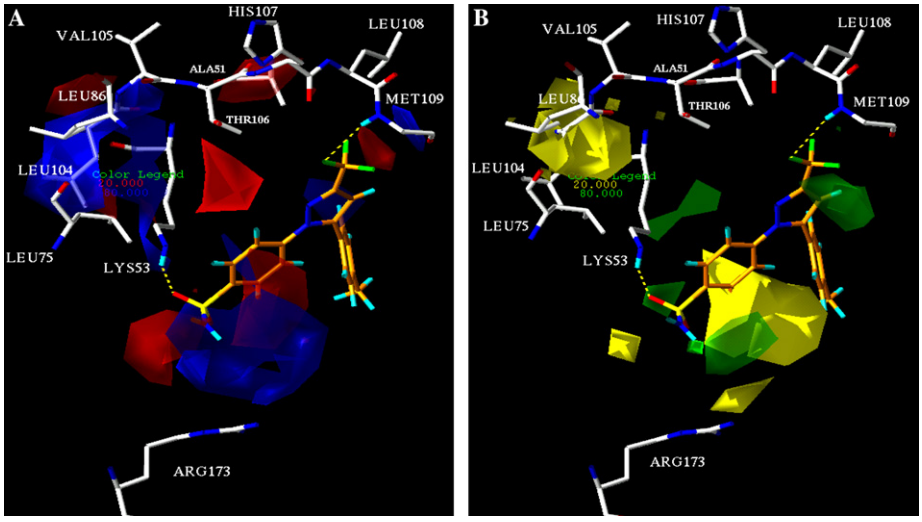

Figure 3. Contour maps of QSAR-3D/CoMFA compared with the topology of celecoxib–p38 MAPK complex. Only the residues within 3 Å around the inhibitor are shown for clarity. (A) Electrostatic contour plots of celecoxib. (B) Steric contour plots of celecoxib. The residues are represented as sticks, and the carbon atoms of the inhibitors are shown in orange (celecoxib), blue (N), red (O), and green (halogen); the yellow dashed lines are the hydrogen bonds formed between celecoxib and p38 MAPK.

Table 1. Docking energies and calculated activities of SB203580 and coxib derivatives in p38 MAP kinase

Compounds	FlexX score (kcal/mol)	IC_{50}[a](μM)
SB203580	−22.2	0.072
Etoricoxib	−18.6	0.53
Celecoxib	−12.4	0.81

[a] Calculated activities based on CoMFA model.

etoricoxib makes four hydrogen bonds with Arg173 (3 hydrogen bonds) and Lys53 (1 hydrogen bond), while celecoxib makes only two hydrogen bonds with amino acid residues present in the same pocket of SB203580 recognition.[19]

The combination of docking and 3D-QSAR/CoMFA results enabled us to propose how the selective COX-2 inhibitor celecoxib could also act by inhibiting p38 MAPK, as speculatively anticipated by Muller. [18] The docking model predicted celecoxib to have a less favorable ΔG_{bind} (−12.4 kcal/mol) in the protein–ligand complex than the p38 MAPK inhibitor SB203580 (−22.2 kcal/mol). The CoMFA model results were indicative that the sulfonamide group and trifluoromethyl group of celecoxib are associated to the regions where negative potential is favorable to the inhibitory activity, in accordance with the docking results, which indicate the formation of hydrogen bonds between these groups and the N–H groups of residues Met109 and Lys53. Unfavorable steric effects associated to the diaryl substitutes were also predicted by the CoMFA model applied to celecoxib. Furthermore, based on binding energies given by the FlexX scoring function and calculated inhibitory activity by the CoMFA models, we also suggested that the p38 activity could be inhibited by etoricoxib, suggesting that these drugs can exert their anti-inflamatory effects as symbiotic agents.

Acknowledgments

The authors are thankful for the financial support from PRONEX, CNPq (Br), and FAPERJ (Br), and fellowships (to EJB, LML, CAMF, CMRS).

Supplementary data

Supplementary data associated with this article can be found in the online version at doi:10.1016/j.bmcl.2005.05.107.

References and notes

1. Lee, J. C.; Laydon, J. T.; McDonnell, P. C.; Gallagher, T. F.; Kumar, S.; Green, D.; McNulty, D.; Blumenthal, M. J.; Heys, J. R.; Landvatter, S. W.; Strickler, J. E.; McLaughlin, M. M.; Siemens, I. R.; Fisher, S. M.; Livi, G. P.; White, J. R.; Adams, J. L.; Young, P. R. *Nature* **1994**, *372*, 739.
2. Chakravarty, S.; Dugar, S. *Annu. Rep. Med. Chem.* **2002**, *37*, 177.
3. Wang, Z.; Canagarajah, B. J.; Boehm, J. C.; Kassisa, S.; Cobb, M. H.; Young, P. R.; Abdel-Meguid, S.; Adams, J. L.; Goldsmith, E. *J. Struct.* **1998**, *6*, 1117.
4. Kumar, S.; Boehm, J.; Lee, J. C. *Nature* **2003**, *2*, 717.
5. Wan, Z.; Boehm, J. C.; Bower, M. J.; Kassis, S.; Lee, J. C.; Zhao, B.; Adams, J. L. *Bioorg. Med. Chem. Lett.* **2003**, *13*, 1191.
6. Szymkowski, D. E. *Drug Discov. Today* **2005**, *10*, 14.
7. Vane, J. R.; Bakhle, Y. S.; Botting, R. M. *Annu. Rev. Pharmacol. Toxicol.* **1998**, *38*, 97.
8. Penning, T. D.; Talley, J. J.; Bertenshaw, S. R.; Carter, J. S.; Collins, P. W.; Docter, S.; Graneto, M. J.; Lee, L. F.; Malecha, J. W.; Miyashiro, J. M.; Rogers, R. S.; Rogier, D. J.; Yu, S. S.; Anderson, G. D.; Burton, E. G.; Cogburn, J. N.; Gregory, S. A.; Koboldt, C. M.; Perkins, W. E.; Seibert, K.; Veenhuizen, A. W.; Zhang, Y. Y.; Isakson, P. C. *J. Med. Chem.* **1997**, *40*, 1347.
9. Friesen, R. W.; Brideau, C.; Chan, C. C.; Charleson, S.; Deschenes, D.; Dube, D.; Ethier, D.; Fortin, R.; Gauthier, J. Y.; Girard, Y.; Gordon, R.; Greig, G. M.; Riendeau, D.; Savoie, C.; Wang, Z. Y.; Wong, E.; Visco, D.; Xu, L. J.; Young, R. N. *Bioorg. Med. Chem. Lett.* **1998**, *8*, 2777.
10. Prasit, P.; Wang, Z.; Brideau, C.; Chan, C. C.; Charleson, S.; Cromlish, W.; Ethier, D.; Evans, J. F.; Ford-Hutchinson, A. W.; Gauthier, J. Y.; Gordon, R.; Guay, J.; Gresser, M.; Kargman, S.; Kennedy, B.; Leblanc, Y.; Léger, S.; Mancini, J.; O'Neill, G. P.; Ouellet, M.; Percival, M. D.; Perrier, H.; Riendeau, D.; Rodger, I.; Tagari, P.; Thérien, M.; Vickers, P.; Wong, E.; Xu, L. I.; Young, R. N.; Zamboni, R.; Boyce, S.; Rupniak, N.; Forrest, N.; Visco, D.; Patrick, D. *Bioorg. Med. Chem.* **1999**, *9*, 1773.
11. Chun, K.; Kim, S. H.; Song, Y. S.; Surh, Y. J. *Carcinogenesis* **2004**, *25*, 713.
12. Pirard, B.; Pickett, S. D. *J. Chem. Inf. Comput. Sci.* **2000**, *40*, 1431.
13. Romeiro, N. C. Ph.D. Thesis, Federal University of Rio de Janeiro, December 2002.
14. Sperandio da Silva, G. M.; Sant'Anna, C. M. R.; Barreiro, E. *J. Bioorg. Med. Chem.* **2004**, *12*, 3159.
15. Sybyl, Version 7.0. Tripos Associates: St. Louis, MO, 2004.
16. Kramer, B.; Rarey, M.; Lengauer, T. *Proteins* **1999**, *37*, 228.
17. Rarey, M.; Kramer, B.; Lengauer, T.; Klebe, G. *J. Mol. Biol.* **1996**, *261*, 470.
18. Müller, G. *Drug Discov. Today* **2003**, *8*, 681.
19. See supplementary data.